Chem Biol Drug Des 2011; **77:** 225–240

Research Article

doi: 10.1111/j.1747-0285.2011.01086.x

Rational Design of α-Helical Antimicrobial Peptides to Target Gram-negative Pathogens, *Acinetobacter baumannii* and *Pseudomonas aeruginosa*: Utilization of Charge, 'Specificity Determinants,' Total Hydrophobicity, Hydrophobe Type and Location as Design Parameters to Improve the Therapeutic Ratio

Ziqing Jiang[1], Adriana I. Vasil[2], Lajos Gera[1], Michael L. Vasil[2] and Robert S. Hodges[1]

[1]*Department of Biochemistry & Molecular Genetics, University of Colorado, School of Medicine, Anschutz Medical Campus, Aurora, CO, 80045, USA*

[2]*Department of Microbiology, University of Colorado, School of Medicine, Anschutz Medical Campus, Aurora, CO, 80045, USA*

**Corresponding author: Robert S. Hodges, robert.hodges@ucdenver.edu*

The rapidly growing problem of increased resistance to classical antibiotics makes the development of new classes of antimicrobial agents with lower rates of resistance urgent. Amphipathic cationic α-helical antimicrobial peptides have been proposed as a potential new class of antimicrobial agents. The goal of this study was to take a broad-spectrum, 26-residue, antimicrobial peptide in the all-D conformation, peptide D1 (K13) with excellent biologic properties and address the question of whether a rational design approach could be used to enhance the biologic properties if the focus was on Gram-negative pathogens only. To test this hypothesis, we used 11 and 6 diverse strains of *Acinetobacter baumannii* and *Pseudomonas aeruginosa*, respectively. We optimized the number and location of positively charged residues on the polar face, the number, location, and type of hydrophobe on the non-polar face and varied the number of 'specificity determinants' in the center of the non-polar face from 1 to 2 to develop four new antimicrobial peptides. We demonstrated not only improvements in antimicrobial activity, but also dramatic reductions in hemolytic activity and unprecedented improvements in therapeutic indices. Compared to our original starting peptide D1 (V13), peptide D16 had a 746-fold improvement in hemolytic activity (i.e. decrease), maintained antimicrobial activity, and improved the therapeutic indices by 1305-fold and 895-fold against *A. baumannii* and *P. aeruginosa*, respectively. The resulting therapeutic indices for D16 were 3355 and 895 for *A. baumannii* and *P. aeruginosa*, respectively. D16 is an ideal candidate for commercialization as a clinical therapeutic to treat Gram-negative bacterial infections.

Key words: *Acinetobacter baumannii*, antimicrobial peptides, Gram-negative pathogens, *Pseudomonas aeruginosa*, specificity determinants

Received 24 November 2010, accepted for publication 31 December 2010

Acinetobacter baumannii and *Pseudomonas aeruginosa* are two increasingly problematic hospital-associated Gram-negative pathogens because of dramatic increases in the incidence of antibiotic-resistant species (1). The mechanisms of resistance to classical antibiotics generally fall into three categories: (i) antimicrobial-inactivating enzymes, (ii) reduced access to bacterial targets, or (iii) mutations that change targets or cellular functions (2,3).

Antimicrobial resistance among *Acinetobacter* species has increased substantially in the past decade (1) and were the only Gram-negative pathogens associated with consistently increasing proportions of hospital-acquired pneumonias, surgical site infection, and urinary tract infection in all hospitals of the National Nosocomial Infections Surveillance System from 1986 to 2003 (1). During this period of time, the proportion of resistance to antibiotics, amikacin (aminoglycoside class), imipenem (β-lactam class), and ceftazidime (ceftazidime class) increased by approximately 4-fold, 20-fold, and 3-fold, respectively (1).

Pseudomonas aeruginosa is a difficult organism to control with antibiotics because of the high intrinsic resistance of these organisms because of their low outer-membrane permeability coupled with secondary resistance mechanisms such as an inducible cephalosporinase or antibiotic efflux pumps (4). The proportion of resistance to imipenem and ceftazidime both increased by approximately 2-fold according to National Nosocomial Infections Surveillance System

from 1986 to 2003 (1). In a recent study, 550 clinical isolates of *A. baumannii* and 250 clinical isolates of *P. aeruginosa* were analyzed for the prevalence of multidrug resistance (5) and it was found that 74% of *A. baumannii* and 34% of *P. aeruginosa* were multidrug resistant.

The mechanisms of resistance in *A. baumannii* and *P. aeruginosa* generally fall into three paths (2,3): (i) reduced access to bacterial targets by either down-regulating the porin channels through which antibiotics enter the cell or by removing antibiotics through multidrug efflux pumps; (ii) antimicrobial-inactivating enzymes such as β-lactamases and aminoglycoside-modifying enzymes; or (iii) mutations that change targets or cellular functions.

The indiscriminate use of broad-spectrum antibiotics in both hospital and community settings creates environments in which resistant pathogenic bacteria have a significant survival advantage (3). Although new antibiotics with new targets may be developed, the above circumstances will still inevitably lead to resistance to classical antibiotics. Effective infection control measures and development of new classes of antimicrobial agents with lower rates of resistance should be continually emphasized and are urgently required.

Amphipathic cationic antimicrobial peptides (AMPs) have been proposed as a potential new class of antibiotics with the ability to kill target cells rapidly, with broad spectrum activity and effectiveness against some of the most serious antibiotic-resistant pathogens isolated in clinics. Cationic AMPs of the α-helical class have two unique features: a net positive charge of at least +2 and an amphipathic character, with a non-polar face and a polar/charged face (6). In our recent review of α-helical AMPs, we found that the vast majority of peptides contain between 3 and 10 positively charged residues with a positive charge density of 1–3 positively charged residues for every 10 residues in the peptide (7). The largest number of amphipathic α-helical AMPs are in the range of 22–27 residues in length (7). Also, it is thought that the development of resistance is considerably reduced with membrane-active peptides whose sole target is the cytoplasmic membrane and whose interactions with membrane components are non-specific. However, even if their sole target is the cell membrane, hemolytic activity or toxicity to mammalian cells is always a potential barrier preventing them from being used as systemic therapeutics.

The goal in the development of antimicrobial peptides is to optimize hydrophobicity, to minimize eukaryotic cell toxicity, and to maximize antimicrobial activity, which in turn optimizes the therapeutic index. The vast majority of native AMPs are very hemolytic. To that end, the introduction of the 'specificity determinant' design concept was developed in our laboratory as a biophysical mechanism to remove toxicity of amphipathic α-helical antimicrobial peptides (as measured by hemolytic activity against human red blood cells). We successfully introduced a 'specificity determinant', a positively charged lysine residue (K13) in the center of the non-polar face of our starting compound, **D1 (V13)** (valine at position 13 in the center of the non-polar face) (Figure 1). This 26-residue amphipathic α-helical antimicrobial peptide without a specificity determinant had excellent antimicrobial activity, but was highly toxic to human red blood cells leading to an unacceptable low therapeutic index. For example, the geometric mean of the minimal inhibitory concentration (MIC) value

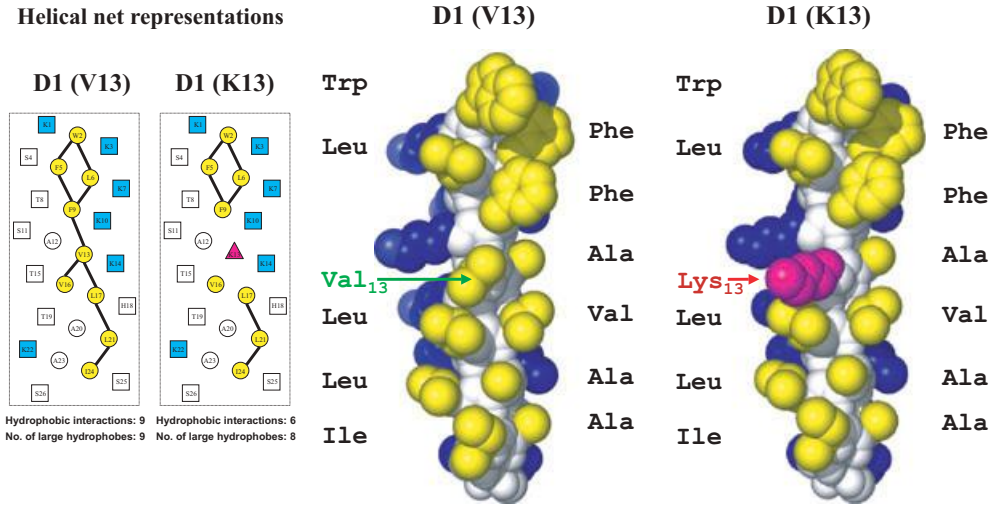

Figure 1: Helical net representation and space-filling model of peptide **D1 (V13)** and **D1 (K13)**. In the helical net (left panel), the one-letter code is used for amino acid residues. The 'specificity determinant' lysine residue at position 13 in the center of the non-polar face of peptide **D1 (K13)** is denoted by a pink triangle. The amino acid residues on the polar face are boxed, and the positively charged lysine residues are colored blue. The amino acid residues on the non-polar face are circled, and the large hydrophobes are colored yellow (Trp, Phe, Leu, Val, and Ile). The $i \rightarrow i + 3$ and $i \rightarrow i + 4$ hydrophobic interactions between large hydrophobes along the helix are shown as black bars. In the space-filling model (right panel), hydrophobic amino acids on the non-polar face are colored yellow; hydrophilic amino acids on the polar face are colored blue; the peptide backbone is colored white. The 'specificity determinant' lysine residue at position 13 in the center of the non-polar face of peptide **D1 (K13)** is colored pink. The models were created with the PyMOL (version 0.99) program.

against a series of Gram-negative and Gram-positive bacteria gave a value of 2.9 and 2.1 μM, respectively. The minimal hemolytic concentration (MHC) gave a value of 5.2 μM. The therapeutic index is the ratio of MHC/MIC; thus, 5.2/2.9 = 1.8 for Gram-negative bacteria and 5.2/2.1 = 2.5 for Gram-positive bacteria (8). We introduced a single substitution of a lysine residue at position 13 and referred to this analog as **D1 (K13)** (Figure 1). This valine-to-lysine substitution in the center of the non-polar face (denoted as 'specificity determinant') achieved the following biophysical characteristics: (i) decreased the number of hydrophobic interactions from 9 to 6 compared to peptide **D1 (V13)** (helical net representation, Figure 1); (ii) disrupted the continuous hydrophobic surface into two separated patches (Figure 1), which in turn resulted in the peptide having no helical structure in aqueous conditions; (iii) reduced the overall hydrophobicity, and (iv) prevented peptide self-association in aqueous condition (8). This substitution also had dramatic effects on biologic activity: (i) reduced toxicity by greater than 32-fold as measured by hemolytic activity against human red blood cells; (ii) enhanced antimicrobial activity by 3-fold for Gram-negative bacteria and (iii) improved the therapeutic index by 90-fold and 17-fold compared to the starting peptide **D1 (V13)** against Gram-negative bacteria and Gram-positive bacteria, respectively (8). Generally speaking, the 'specificity determinant' design technique allowed our antimicrobial peptides to discriminate between eukaryotic and prokaryotic cell membranes, that is, exhibit pronounced selectivity for prokaryotic cell membranes. This effect has also been recently validated by another group who resynthesized our two key peptides, **D1 (V13)** and **D1 (K13)**, and also demonstrated the importance of a positively charged residue ('specificity determinant') in the non-polar face of a native 16-residue antimicrobial peptide, RTA3, derived from *Streptococcus mitis* (9).

We have also demonstrated that the sole target of **D1 (K13)** was the membrane, and its interactions with the membrane did not involve a stereoselective interaction with a chiral enzyme, lipid or protein receptor because the all-L and all-D conformations had similar biologic and biophysical properties (10). Thus, the peptide could be prepared in the all-D conformation, which is completely resistant to proteolytic enzyme degradation and which enhances the potential of **D1 (K13)** as a clinical therapeutic (8,10). We have also demonstrated the role of hydrophobicity and importance of net positive charge on antimicrobial and hemolytic activity (11,12). In addition, we have shown that there is a threshold hydrophobicity at which optimal antimicrobial activity can be obtained. That is, decreasing peptide hydrophobicity on the non-polar face reduces antimicrobial activity, while increasing peptide hydrophobicity improves antimicrobial activity to a point until an optimum is reached, and further increases in hydrophobicity beyond the optimum can decrease antimicrobial activity (11). This effect is likely due to increased peptide dimerization, which prevents peptide access to the membrane in prokaryotic cells. Peptide dimers in their folded α-helical conformation would be inhibited from passing through the capsule and cell wall to reach the target membrane, unlike a less hydrophobic unstructured monomer. Thus, hydrophobicity affects the unstructured monomer to folded dimer equilibrium and antimicrobial activity. Interestingly, increasing hydrophobicity on the non-polar face of antimicrobial peptides results in stronger hemolysis of erythrocytes, which supports the view that compositional differences between prokaryotic and eukaryotic cells (capsule, cell wall and membrane lipid composition) have dramatic effects on the role hydrophobicity plays on antimicrobial and hemolytic activity.

We have shown that **D1 (K13)** because of its antimicrobial activities including antibacterial (Gram-negative and Gram-positive), antifungal, and antituberculosis activities along with other desired biologic and biophysical properties has potential as a broad-spectrum therapeutic (8,10,11,13,14). However, the question remained, 'Could an antimicrobial peptide with enhanced biologic properties be rationally designed if the focus was on Gram-negative pathogens only, rather than broad-spectrum activity?' In this study, we chose two Gram-negative pathogens: *A. baumannii* (11 isolates) and *P. aeruginosa* (six isolates) to evaluate antimicrobial peptide activity. We used peptide **D1 (K13)** as the starting peptide for optimizing the number and location of positively charged residues on the polar face, the number of 'specificity determinants' on the non-polar face and overall hydrophobicity on the non-polar face including type and location of hydrophobes. We were able to develop four new antimicrobial peptides with improvements in antimicrobial activity against Gram-negative pathogens and dramatic reductions in hemolytic activity and unprecedented improvements in therapeutic indices.

Experimental Procedures

Peptide synthesis and purification

Synthesis of the peptides was carried out by standard solid-phase peptide synthesis methodology using t-butyloxycarbonyl (t-Boc) chemistry and 4-methylbenzhydrylamine resin (substitution level 0.97 mmol/g) followed by cleavage of the peptide from the resin as described previously (8,10,11). Peptide purification was performed by reversed-phase high-performance liquid chromatography (RP-HPLC) on a Zorbax 300 SB-C_8 column (250 $\times$ 9.4 mm I.D.; 6.5 μm particle size, 300 Å pore size; Agilent Technologies, Little Falls, DE, USA) with a linear AB gradient (0.1% acetonitrile/min) at a flow rate of 2 mL/min, where eluent A was 0.2% aqueous trifluoroacetic acid (TFA), pH 2, and eluent B was 0.18% TFA in acetonitrile, where the shallow 0.1% acetonitrile/min gradient started 12% below the acetonitrile concentration required to elute the peptide on injection of analytical sample using a gradient of 1% acetonitrile/min (15).

Analytical RP-HPLC and temperature profiling of peptides

The purity of the peptides was verified by analytical RP-HPLC, and the peptides were characterized by mass spectrometry (LC/MS). Crude and purified peptides were analyzed on an Agilent 1100 series liquid chromatograph (Little Falls, DE, USA). Runs were performed on a Zorbax 300 SB-C_8 column (150 $\times$ 2.1 mm I.D.; 5 μm particle size, 300 Å pore size) from Agilent Technologies using a linear AB gradient (1% acetonitrile/min) and a flow rate of 0.25 mL/min, where eluent A was 0.2% aqueous TFA, pH 2, and eluent B was 0.18% TFA in acetonitrile. Temperature profiling analyses were performed on the same column in 3 °C increments, from 5 to 80 °C using a linear AB gradient of 0.5% acetonitrile/min, as described previously (8,10,11,16).

Characterization of helical structure

The mean residue molar ellipticities of peptides were determined by circular dichroism (CD) spectroscopy, using a Jasco J-815 spectropolarimeter (Jasco Inc. Easton, MD, USA) at 5 °C under benign (non-denaturing) conditions (50 mM NaH_2PO_4/Na_2HPO_4/100 mM KCl, pH 7.0), hereafter referred to as benign buffer, as well as in the presence of an α-helix-inducing solvent, 2,2,2-trifluoroethanol, TFE (50 mM NaH_2PO_4/Na_2HPO_4/100 mM KC1, pH 7.0 buffer/50% TFE). A 10-fold dilution of an approximately 500-μM stock solution of the peptide analogs was loaded into a 0.1-cm quartz cell and its ellipticity scanned from 195 to 250 nm. Peptide concentrations were determined by amino acid analysis.

Determination of peptide amphipathicity

Amphipathicity of peptides were determined by the calculation of hydrophobic moment (17), using the software package Jemboss version 1.2.1 (18), modified to include a hydrophobicity scale determined in our laboratory (19,20). The hydrophobicity scale used in this study is listed as follows: Trp, 33.0; Phe, 30.1; Leu, 24.6; Ile, 22.8; Met, 17.3; Tyr, 16.0; Val, 15.0; Pro, 10.4; Cys, 9.1; His, 4.7; Ala, 4.1; Thr, 4.1; Arg, 4.1; Gln, 1.6; Ser, 1.2; Asn, 1.0; Gly, 0.0; Glu, −0.4; Asp, −0.8; and Lys, −2.0. These hydrophobicity coefficients were determined from reversed-phase chromatography at pH7 (10 mM PO_4 buffer containing 50 mM NaCl) of a model random-coil peptide with a single substitution of all 20 naturally occurring amino acids (19). We proposed that this HPLC-derived scale reflects the relative difference in hydrophilicity/hydrophobicity of the 20 amino acid sidechains more accurately than previously determined scales [see recent review where this scale was compared to other scales (20)].

Gram-negative bacteria strains used in this study

All the *A. baumannii* strains used in this study were either obtained from the collection of Dr. Anthony A. Campagnari at the University of Buffalo or originally isolated from different patients and organs/tissues: strain 649, blood; strain 689, groin; strain 759, gluteus; strain 821, urine; strain 884, axilla; strain 899, perineum; strain 964, throat; strain 985, pleural fluid and strain 1012, sputum; or were purchased from the American Type Culture Collection (ATCC, Manassas, VA, USA); strain ATCC 17978, fatal meningitis; and strain ATCC 19606, urine.

Pseudomonas aeruginosa strains used are as follows: strain PAO1 was isolated from a human wound in 1955 in Australia (21); strain WR5 was isolated from a burn patient at Walter Reed Army Hospital, Washington, DC, in 1976 and is a natural *toxA*$^-$ mutant but is virulent in experimental mouse models (22,23); strain PAK was originally isolated at Memorial University, St. John's, Newfoundland, Canada, and is widely used in the analysis of pili (24,25); strain PA14 was originally isolated as a clinical isolate in 1995 at the Massachusetts General Hospital, Boston, and is virulent in a variety of plant and animal models of infection (26); strain M2 was originally isolated in 1975 from the gastrointestinal tract of a healthy CF1 mouse, University of Cincinnati College of Medicine, and Shriners Burns Institute, Cincinnati, OH, and is virulent in a burn mouse model of *P. aeruginosa* infection(27); and strain CP204 was isolated from a patient with cystic fibrosis in 1989 at the National Jewish Medical and Research Center, Denver, CO. All strains have been maintained at −80 °C in the laboratory of Michael Vasil.

Measurement of antimicrobial activity

Measurement of antimicrobial activity (MICs) was determined by a standard microtiter dilution method in Mueller–Hinton (MH) medium. Briefly, cells were grown overnight at 37 °C in MH broth and were diluted in the same medium. Serial dilutions of the peptides were added to the microtiter plates in a volume of 50 μL, followed by the addition of 50 μL of bacteria to give a final inoculum of 5×10^5 colony-forming units (CFU)/mL. The plates were incubated at 37 °C for 24 h, and the MICs were determined as the lowest peptide concentration that inhibited growth.

Measurement of hemolytic activity (HC_{50})

The length of time erythrocytes are exposed to AMPs during the hemolysis assay is the least standardized parameter of the method. Reported protocols have exposures ranging from 10 min (28) to 24 h (28,29). The most commonly cited times are 30 min (30–32) and 1 h (33–35). Such short exposures provide valuable information about relative acute toxicity across a peptide series. However, higher exposure times are necessary to evaluate the longer-term toxicity that could result if AMPs are not fully metabolized and cleared within 1 h *in vivo*. Therefore, we suggest hemolysis should be measured using a time–course approach extending to at least 18 h of exposure time.

Peptide samples (concentrations determined by amino acid analysis) were added to 1% human erythrocytes in phosphate-buffered saline (100 mM NaCl, 80 mM Na_2HPO_4, 20 mM NaH_2PO_4, pH 7.4), and the reaction mixtures were incubated at 37 °C for 18 h in microtiter plates. Twofold serial dilutions of the peptide samples were carried out. This determination was made by withdrawing aliquots from the hemolysis assays and removing unlysed erythrocytes by centrifugation ($800 \times g$). Hemoglobin release was determined spectrophotometrically at 570 nm. The control for 100% hemolysis was a sample of erythrocytes treated with water. The control for no release of hemoglobin was a sample of 1% erythrocytes without any peptide added. Because erythrocytes were in an isotonic medium, no detectable release (<1% of that released upon complete hemolysis) of hemoglobin was observed from this control during the course of the assay. The hemolytic activity was determined as the peptide concentration that caused 50% hemolysis of erythrocytes after 18 h (HC_{50}). HC_{50} was determined from a plot of percent lysis versus peptide concentration. When a HC_{50} value could not be measured at 1000 μg/mL, an estimated value was obtained by linear extrapolation of the slope of the line between 500 and 1000 μg/mL (Figure 6). For example, D16 showed only 10.7% lysis after 18 h at 1000 μg/mL.

Calculation of therapeutic index (HC_{50}/MIC ratio)

The therapeutic index is a widely accepted parameter to represent the specificity of antimicrobial peptides for prokaryotic versus

eukaryotic cells. It is calculated by the ratio of HC_{50} (hemolytic activity) and MIC (antimicrobial activity); thus, larger values of therapeutic index indicate greater specificity for prokaryotic cells.

Results

In this study, we designed and synthesized five new antimicrobial peptides as analogs of our starting 26-residue peptide **D1 (V13)** and our lead broad-spectrum peptide **D1 (K13)**. The five analogs involve a minimum of six to a maximum of 12 substitutions in the sequence of peptide **D1 (V13)** (Table 1). Figures 2 and 3 show the amino acid sequences in helical net representations. The polar faces (top panels) display the polar face residues along the center of the helical net and are boxed (positively charged residues are colored blue). The non-polar faces (bottom panels) display the non-polar residues along the center of the helical net and are circled with the large hydrophobes colored green (Trp, Phe, Val, and Ile) and yellow (Leu). The positively charged residue(s) in the center of the non-polar face (specificity determinant(s)) are denoted as pink triangles. The potential i to $i + 3/i$ to $i + 4$ electrostatic repulsions between positively charged residues are shown as black dotted lines. The i to $i + 3/i$ to $i + 4$ hydrophobic interactions between large hydrophobes are shown as solid black lines. These representations allow easy comparison of different analogs to explain their biologic and biophysical properties described later.

Peptide hydrophobicity

RP-HPLC of peptides is a particularly good method to characterize overall peptide hydrophobicity, and the retention times of peptides are highly sensitive to the conformational status of peptides upon interaction with the hydrophobic environment of the column matrix (8,36). The non-polar face of an amphipathic α-helical peptide represents a preferred binding domain for interaction with the hydrophobic matrix of a reversed-phase column (37).

Peptide secondary structure

Figure 4 shows the CD spectra of the peptides in different environments, i.e., under benign (non-denaturing) conditions (50 mM NaH_2PO_4/Na_2HPO_4/100 mM KCl, pH 7.0; Figure 4A) and in buffer with 50% 2,2,2-trifluoroethanol (TFE) to mimic the hydrophobic environment of the membrane (Figure 4B). It should be noted that the all-D conformation of the peptides show CD spectra that are exact mirror images compared to their L enantiomers, with ellipticities equivalent but of opposite sign (10). All the peptides except **D22** and **D1 (V13)** showed negligible secondary structure in benign buffer (Figure 4A and Table 2). **D1 (V13)** showed the most helical structure in benign conditions because of its uninterrupted hydrophobic surface along the non-polar face of the molecule, which stabilizes the helical structure. **D22** exhibited a slight α-helical spectrum under benign conditions (Figure 4A) compared to the spectra of the other analogs. A highly helical structure was induced by the non-polar environment of 50% TFE, a mimic of hydrophobicity and the α-helix-inducing ability of the membrane (Figure 4B and Table 2). All the peptide analogs in 50% TFE showed a typical α-helix spectrum with double maxima at 208 and 222 nm. The helicities of the peptides in benign buffer and in 50% TFE relative to

Table 1: Peptides used in this study

Peptide Name	Substitution[a]	Sequence[b] 1 13 16 26
D1 (V13)		Ac-K-W-K-S-F-L-K-T-F-K-S-A-V-K-T-V-L-H-T-A-L-K-A-I-S-S-amide
D1 (K13)	D-(V13K)	Ac-K-W-K-S-F-L-K-T-F-K-S-A-**K**-K-T-V-L-H-T-A-L-K-A-I-S-S-amide
D11	D-(V13K, K10S, S11K, T15K, H18K, S26K)	Ac-K-W-K-S-F-L-K-T-F-S-K-A-**K**-K-K-V-L-K-T-A-L-K-A-I-S-K-amide
D22	D-(V13K, V16A, K10S, S11K, T15K, H18K, A20L, S26K)	Ac-K-W-K-S-F-L-K-T-F-S-K-A-**K**-K-K-A-L-K-T-L-L-K-A-I-S-K-amide
D14	D-(V13K, V16K, K10S, S11K, T15K, H18K, A20L, S26K)	Ac-K-W-K-S-F-L-K-T-F-S-K-A-**K**-K-K-**K**-L-K-T-I-L-K-A-I-S-K-amide
D15	D-(V13K, V16L, W2L, F5L, F9L, K10S, S11K, T15K, H18K, I24L, S26K)	Ac-K-L-K-S-L-L-K-T-L-S-K-A-**K**-K-K-L-L-K-T-A-L-K-A-L-S-K-amide
D16	D-(V13K, V16K, W2L, F5L, F9L, K10S, S11K, T15K, H18K, A20L, I24L, S26K)	Ac-K-L-K-S-L-L-K-T-L-S-K-A-**K**-K-K-**K**-L-K-T-L-L-K-A-L-S-K-amide
Control C		Ac-E-L-E-K-G-G-L-E-G-E-K-G-G-K-E-L-E-K-amide

[a]The D denotes that all amino acid residues in each peptide are in the D conformation, except for the control peptide, which is in the all L conformation.
[b]Peptide sequences are shown using the one-letter code for amino acid residues; Ac denotes N^{α}-acetyl; and -amide denotes C^{α}-amide. The 'specificity determinant(s)', Lys residues incorporated in the center of the non-polar face are given in bold (position 13 or positions 13 and 16).

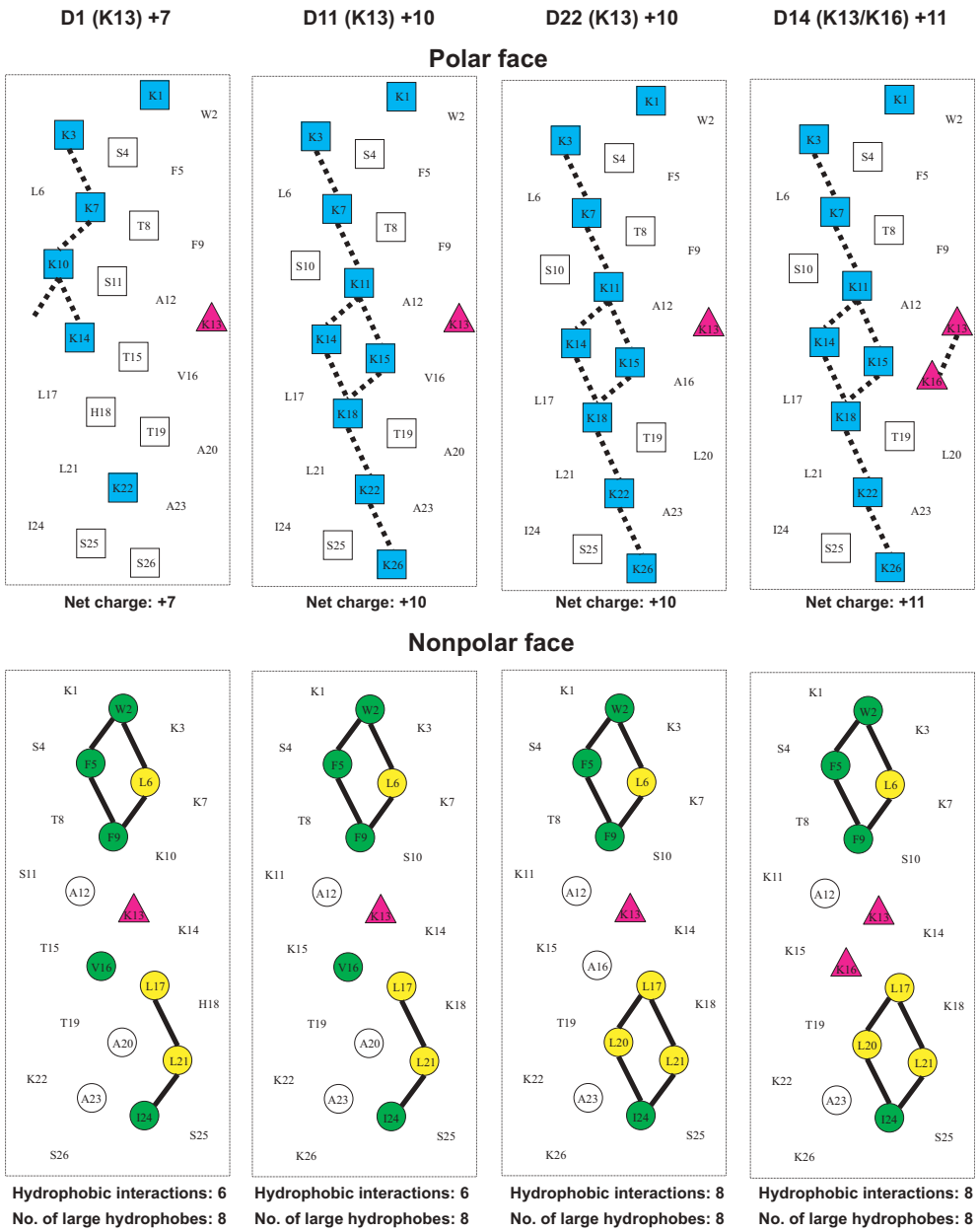

Figure 2: Helical net representation of peptides **D1 (K13)**, **D11**, **D22**, and **D14**. The one-letter code is used for amino acid residues. D denotes that all residues in the peptides are in the D conformation. The 'specificity determinant(s)' lysine residue(s) at position 13 only or positions 13 and 16 in the center of the non-polar face is denoted by a pink triangle(s). The amino acid residues on the polar face are boxed, and the positively charged lysine residues are colored blue. The potential $i \rightarrow i + 3$ and $i \rightarrow i + 4$ electrostatic repulsions between positively charged residues along the helix are shown as dotted bars. The amino acid residues on the non-polar face are circled; the large hydrophobes other then leucine residues (Trp, Phe, Val, and Ile) are colored green, and the leucine residues are colored yellow. The $i \rightarrow i + 3$ and $i \rightarrow i + 4$ hydrophobic interactions between large hydrophobes along the helix are shown as black bars.

that of peptide **D15** (taken as 100% helix) in 50% TFE were determined (Table 2).

Peptide self-association

Peptide self-association (i.e. the ability to oligomerize/dimerize) in aqueous solution is a very important parameter for antimicrobial activity (8,10,11). We assume that monomeric random-coil antimicrobial peptides are best suited to pass through the capsule and cell wall of microorganisms prior to penetration into the cytoplasmic membrane, induction of α-helical structure, and disruption of membrane structure to kill target cells (11). Thus, if the self-association ability of a peptide in aqueous media is too strong (e.g. forming stable folded dimers/oligomers through interaction of their non-

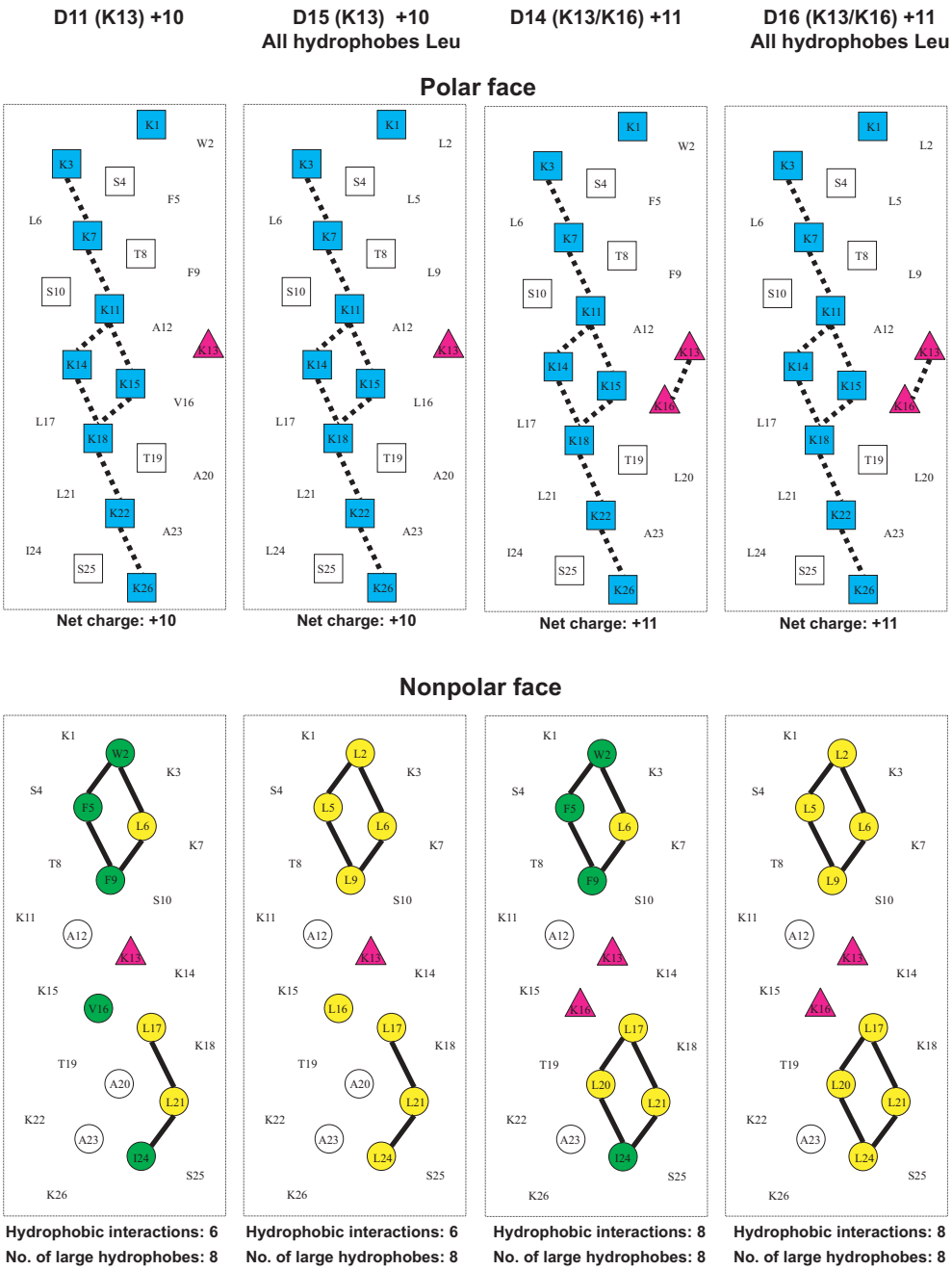

Figure 3: Helical net representation of peptides **D11**, **D15**, **D14**, and **D16**. The one-letter code is used for amino acid residues. D denotes that all residues in the peptides are in the D conformation. The 'specificity determinant(s)' lysine residues at position 13 only or at positions 13 and 16 in the center of the non-polar face is denoted by a pink triangle(s). The amino acid residues on the polar face are boxed, and the positively charged lysine residues are colored blue. The potential $i \rightarrow i + 3$ and $i \rightarrow i + 4$ electrostatic repulsions between positively charged residues along the helix are shown as dotted bars. The amino acid residues on the non-polar face are circled; the large hydrophobes other then leucine residues (Trp, Phe, Val and Ile) are colored green, and the leucine residues are colored yellow. The $i \rightarrow i + 3$ and $i \rightarrow i + 4$ hydrophobic interactions between large hydrophobes along the helix are shown as black bars.

polar faces), this could decrease the ability of the peptide to dissociate to monomer where the dimer cannot effectively pass through the capsule and cell wall to reach the membrane (11). The ability of the peptides in this study to self-associate was determined by the technique of reversed-phase high-performance liquid chromatography (RP-HPLC) temperature profiling at pH 2 over the temperature range of 5–80 °C (16,38,39). The reason pH 2 is used to determine self-association of cationic AMPs is that highly positively charged

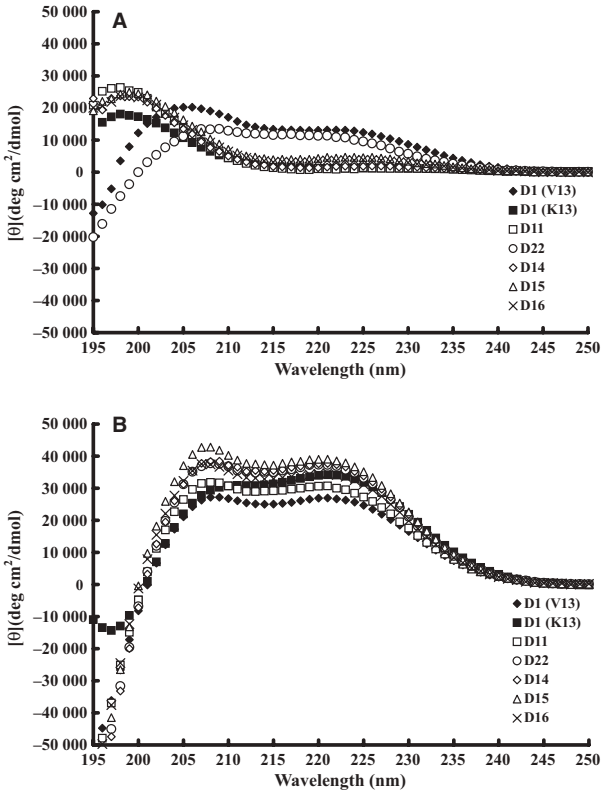

Figure 4: Circular dichroism (CD) spectra. Panel A shows the CD spectra of peptides in aqueous benign buffer (100 mM KCl, 50 mM NaH_2PO_4/Na_2HPO_4 at pH 7.0, 5 °C, and panel B shows the spectra in the presence of buffer-trifluoroethanol (TFE) (1:1, v/v).

peptides are frequently not eluted from reversed-phase columns at pH 7 because of non-specific binding to negatively charged silanols on the column matrix. This is not a problem at pH 2 because the silanols are protonated (i.e. neutral) and non-specific electrostatic interactions are eliminated. At pH 2, the interactions between the peptide and the reversed-phase matrix involve ideal retention behavior, i.e. only hydrophobic interactions between the preferred binding domain (non-polar face) of the amphipathic molecule and the hydrophobic surface of the column matrix are present (37). Figure 5A shows the retention behavior of the peptides after normalization to their retention times at 5 °C. Control peptide C shows a linear decrease in retention time with increasing temperature and is representative of peptides that have no ability to self-associate during RP-HPLC. Control peptide C is a monomeric random-coil peptide in both aqueous and hydrophobic media; thus, its linear decrease in peptide retention behavior with increasing temperature within the range of 5–80 °C represents only the general effects of temperature because of greater solute diffusivity and enhanced mass transfer between the stationary and mobile phase at higher temperatures (40). To allow for these general temperature effects, the data for the control peptide was subtracted from each temperature profile as shown in Figure 5B. Thus, the peptide self-association parameter, P_A, represents the maximum change in peptide retention time relative to the random-coil peptide C. Note that the higher the P_A value, the greater the self-association. The P_A value varies from the lowest value of 2.78 for peptide **D1 (K13)** to the highest value of 7.40 for peptide D15 (Table 2). Peptide **D1 (V13)**, the original starting peptide, has the second highest P_A value and an overall hydrophobicity of 102.5 min compared to **D15** with a value of 93.0 min.

Hemolytic activity

The hemolytic activities of the peptides against human erythrocytes were determined as a measure of peptide toxicity toward higher eukaryotic cells. The effect of peptide concentration on erythrocyte hemolysis is shown in Figure 6. From these plots, the peptide concentration that produced 50% hemolysis was determined (HC_{50}). Peptide **D1 (V13)** was the most hemolytic with a HC_{50} value of

Table 2: Biophysical data of D1 analogs

		Hydrophobicity		Benign		50% TFE			
Peptide name	Net charge	t_R[a] (min)	Δt_R (X-D1(V13))[b] (min)	$[\theta]_{222}$[c]	%Helix[d]	$[\theta]_{222}$[c]	%Helix[d]	P_A[e]	Amphipathicity[f]
D1 (V13)	+6	102.5	0	13 150	34	26 650	71	7.14	5.56
D1 (K13)	+7	76.8	−25.7	1150	3	34 100	88	2.78	4.92
D11	+10	85.4	−17.1	900	2	30 000	78	3.31	5.57
D22	+10	90.7	−11.8	10 900	28	37 000	96	5.13	6.07
D14	+11	81.8	−20.7	1750	5	37 350	97	3.07	5.92
D15	+10	93.0	−9.5	4350	11	38 550	100	7.40	5.29
D16	+11	83.6	−18.9	3550	9	34 150	89	5.17	5.42

[a]t_R denotes retention time in RP-HPLC at pH 2 and room temperature and is a measure of overall peptide hydrophobicity.

[b]Δt_R (X-**D1 (V13)**) is the difference in retention time between the peptide analogs and peptide **D1 (V13)**, as a measure of the change in hydrophobicity.

[c]The mean residue molar ellipticities $[\theta]_{222}$ (deg cm^2/dmol) at wavelength 222 nm were measured at 5 °C in benign conditions (100 mM KCl, 50 mM NaH_2PO_4/Na_2HPO_4, pH 7.0) or in benign buffer containing 50% trifluoroethanol (TFE) by circular dichroism spectroscopy.

[d]The helical content (as a percentage) of a peptide relative to the molar ellipticity value of peptide **D15** in the presence of 50% TFE.

[e]P_A denotes oligomerization/dimerization parameter of each peptide during RP-HPLC temperature profiling, which is the maximal retention time difference of (t_R^t–t_R^5 for peptide analogs) – (t_R^t–t_R^5 for control peptide C) within the temperature range; t_R^t–t_R^5 is the retention time difference of a peptide at a specific temperature (t_R^t) compared with that at 5 °C (t_R^5). The sequence of control peptide C is shown in Table 1.

[f]Amphipathicity was determined by calculation of hydrophobic moment (17) using hydrophobicity coefficients determined by reversed-phase chromatography (19,20); see methods for details.

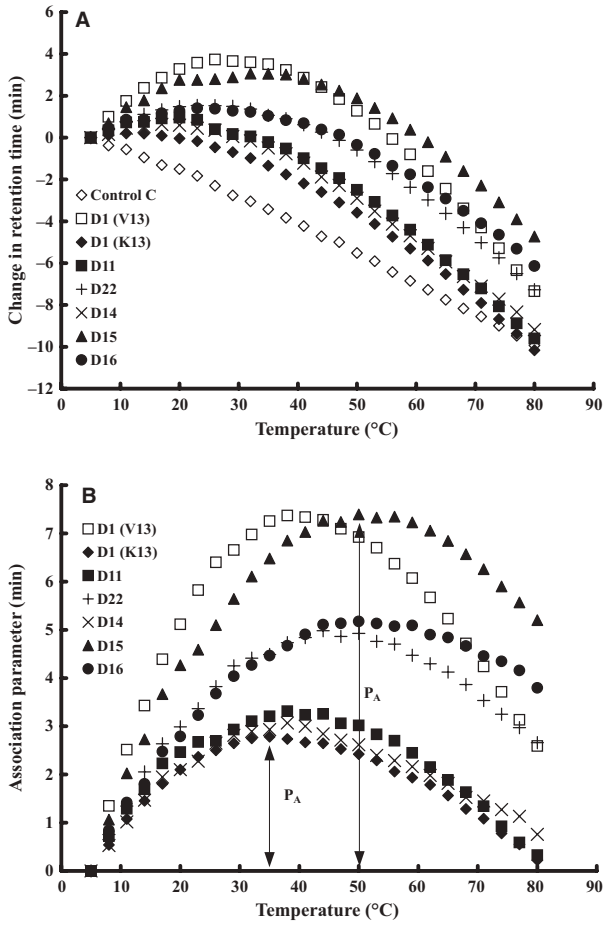

Figure 5: Peptide self-association ability as monitored by temperature profiling in reversed-phase chromatography (RP-HPLC). In panel A, the retention time of peptides are normalized to 5 °C through the expression (t_R^t–t_R^5), where t_R^t is the retention time at a specific temperature of an antimicrobial peptide or control peptide C, and t_R^5 is the retention time at 5 °C. In panel B, the retention behavior of the peptides was normalized to that of control peptide C through the expression (t_R^t–t_R^5 for peptides)–(t_R^t-t_R^5 for control peptide C). The maximum change in retention time from the control peptide C defines the peptide association parameter, denoted P_A (Table 2). The sequences of the peptides and the random-coil control peptide are shown in Table 1.

1.8 μM compared to peptide **D16** where a HC_{50} value could not be determined.

Comparison of Peptides

To best understand the structure–activity relationship in our designs, we compared small groups of peptides with their structures and corresponding activities.

Peptides D1 (K13) versus D11

These peptides were designed with a different net charge and charge distribution on the polar face (Figure 2). Both peptides have

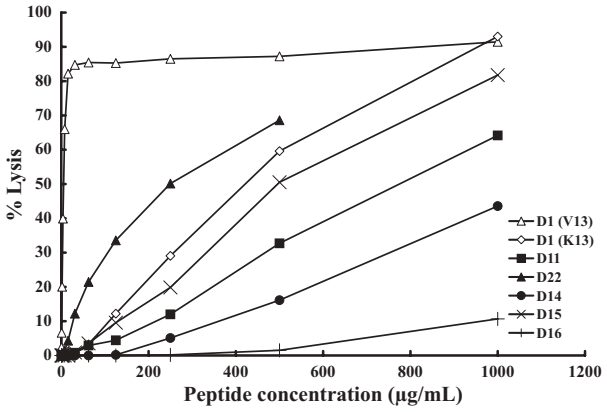

Figure 6: The hemolytic activity of peptide **D1** and analogs. The concentration–response curves of peptides for percentage lysis of human red blood cells (hRBC) are shown. The peptide concentration is in microgram/ml. Peptide **D16** caused only 10.7% lysis after 18 h at 1000 μg/ml.

identical non-polar faces: eight large hydrophobes, six hydrophobic interactions, and one 'specificity determinant' at position 13 (K13); but different polar faces: **D1 (K13)** has a net positive charge of +7 and **D11** has a net positive charge of +10 with a cluster of four positively charged residues in the center of the polar face (K11, K14, K15, and K18) plus an extended narrow strip of positively charged residues (K3 and K7 at the N-terminal of the polar face and K22 and K26 at the C-terminal of polar face). The position of positively charged residues K1, K3, K7, K14, and K22 are identical in both peptides. K10 in peptide **D1 (K13)** is replaced by S10 in peptide **D11**, T15 in peptide **D1 (K13)** is replaced by K15 in peptide **D11**, H18 is replaced by K18 in peptide **D11**, and S26 is replaced by K26 in peptide **D11** (Figure 2). This dramatic change in the polar face increased overall peptide hydrophobicity (76.8 min for peptide **D1 (K13)** to 85.4 min for peptide **D11**), amphipathicity [4.92 for peptide **D1 (K13)** to 5.57 for peptide **D11**] and association parameter [2.78 for peptide **D1 (K13)** to 3.31 for peptide **D11**] (Table 2). This change in the polar face enhanced antimicrobial activity of **D11** against *A. baumannii* (geometric mean of MIC for the 11 different strains) by 1.8-fold and *P. aeruginosa* (geometric mean of MIC for the 6 different strains) by 2.6-fold compared to **D1 (K13)** (Table 3). Hemolytic activity decreased (i.e. improved) by 1.8-fold (Table 4). Overall, the therapeutic index increased by 3.3-fold against *A. baumannii* and 4.6-fold for *P. aeruginosa*. (Table 4). Thus, **D11** has a significant improvement over **D1 (K13)**. **D11** has the poorest hemolytic activity among our D analogs, which has only one 'specificity determinant' (a single lysine residue in the center of the non-polar face, K13). These results suggest that enhancing the positive charge on the polar face from +7 to +10 improved the therapeutic index.

Peptides D11 versus D22

These peptides were designed with a subtle difference in hydrophobicity (Figure 2). Both peptides have identical polar faces: the positively charged cluster in the center and an extended narrow strip of positively charged residues as described earlier. Each peptide has one specificity determinant (K13) on their non-polar face, but **D22**

Table 3: Antimicrobial activity of D1 analogs against *Acinetobacter baumannii* (A) and *Pseudomonas aeruginosa* strains (B) compared to peptide **D1 (V13)**

	Antimicrobial activity against *Acinetobacter baumannii*												
	MIC(μM)[a]												
Peptide name	ATCC 17978	ATCC 19606	649	689	759	821	884	899	964	985	1012	GM[b]	Fold[c]
A)													
D1 (V13)	0.7	0.7	0.7	0.7	0.7	0.7	0.7	0.7	1.3	0.7	0.7	0.7	1.0
D1 (K13)	0.8	1.5	0.8	0.8	1.5	1.5	1.5	1.5	1.5	0.8	0.8	1.1	0.6
D11	0.7	0.7	0.3	0.7	0.3	0.7	0.3	0.3	1.3	0.7	1.3	0.6	1.2
D22	0.7	1.3	1.3	1.3	0.7	0.7	0.7	0.7	0.7	0.7	0.7	0.8	0.9
D14	1.2	0.6	0.6	1.2	0.6	1.2	0.6	0.6	1.2	0.6	0.6	0.8	0.9
D15	0.7	0.7	0.3	0.7	0.3	0.3	0.7	0.7	0.7	0.3	0.7	0.5	1.4
D16	0.7	0.7	0.3	0.3	0.7	0.3	0.3	0.3	0.7	0.3	0.3	0.4	1.8

	Antimicrobial activity against *Pseudomonas aeruginosa*							
	MIC(μM)[a]							
Peptide name	PAO1	PA14	PAK	M2	WR5	CP204	GM[b]	Fold[c]
B)								
D1 (V13)	1.3	1.3	2.6	2.6	1.3	2.6	1.8	1.0
D1 (K13)	2.6	5.2	5.2	2.6	5.2	5.2	4.1	0.4
D11	1.3	1.3	2.6	1.3	1.3	2.6	1.6	1.1
D22	1.3	0.2	1.3	5.1	10.2	10.2	2.3	0.8
D14	2.5	2.5	2.5	5.0	2.5	1.2	2.5	0.7
D15	1.3	0.7	1.3	0.7	1.3	0.7	1.0	1.8
D16	1.3	0.7	2.6	2.6	1.3	1.3	1.5	1.2

[a]Measurement of antimicrobial activity (MIC) is minimal inhibitory concentration that inhibited growth of different strains in Mueller–Hinton (MH) medium at 37 °C after 24 h. MIC is given based on three sets of determinations.
[b]GM, geometric mean of the MIC values.
[c]The fold improvement in antimicrobial activity (geometric mean data) compared to that of **D1 (V13)**.

Table 4: Summary of biologic activity of D1 (V13) analogs

	Hemolytic activity		Antimicrobial activity					
			Acinetobacter baumannii			*Pseudomonas aeruginosa*		
Peptide name	HC_{50}[a] (μM)	Fold[b]	MIC_{GM}[c] (μM)	Therapeutic index[d]	Fold[e]	MIC_{GM}[c] (μM)	Therapeutic index[d]	Fold[e]
D1 (V13)	1.8	1.0	0.7	2.57	1.0	1.8	1.0	1.0
D1 (K13)	140.9	78.3	1.1	**128.1**	49.8	4.1	34.4	34.4
D11	**254.1**	**141.2**	0.6	**423.5**	164.8	1.6	**158.8**	**158.8**
D22	81.3	45.2	0.8	**101.6**	39.5	2.3	35.3	35.3
D14	**351.5**	**195.3**	0.8	**439.4**	171.0	2.5	**140.6**	**140.6**
D15	**169.6**	**94.2**	0.5	**339.2**	132.0	1.0	**169.6**	**169.6**
D16	**1342.0**[f]	**745.6**	0.4	**3355.0**	1305.4	1.5	**894.7**	**894.7**

[a]HC_{50} is the concentration of peptide that results in 50% hemolysis after 18 h at 37 °C. The hemolytic activities that are better than the lead peptide **D1 (K13)** are given in bold.
[b]The fold improvement in HC_{50} compared to that of **D1 (V13)**.
[c]Measurement of antimicrobial activity (MIC) is the minimum inhibitory concentration of peptide that inhibits growth of bacteria after 24 h at 37 °C. MIC_{GM} is the geometric mean of the MIC values from 11 different isolates of *A. baumannii* or six different isolates of *P. aeruginosa*.
[d]Therapeutic index is the ratio of the HC_{50} value (μM) over the geometric mean MIC value (μM). Large values indicate greater antimicrobial specificity. The therapeutic indices with values ≥100 for *A. baumannii* and *P. aeruginosa* are given in bold.
[e]The fold improvement in therapeutic index compared to that of **D1 (V13)**.
[f]The percent lysis for peptide **D16** was only 10.7% after 18 h. We estimated the HC_{50} value based on linear extrapolation of the slope of the line between 500 and 1000 μg/mL (Figure 6). The HC_{50} could be much larger.

has more hydrophobic interactions (six for peptide **D11** and 8 for peptide **D22** and the same number of large hydrophobes (8) with V16 in peptide **D11** changed to A16 in peptide **D22** and A20 in peptide **D11** changed to L20 in peptide **D22**). These changes are in the C-terminal half of the molecules creating two similar separated hydrophobic clusters in peptide **D22** compared to peptide **D11** (Figure 2).

These substitutions increased overall peptide hydrophobicity (85.4 min for peptide **D11** to 90.7 min for peptide **D22**) and amphipathicity (5.57 for peptide **D11** to 6.07 for peptide **D22**) (Table 2). A large increase in the association parameter was observed: from 3.31 for peptide **D11** to 5.13 for peptide **D22** (Table 2).

Peptides **D11** and **D22** have very similar antimicrobial activity against *A. baumannii* (0.6 versus 0.8 μM, respectively) and *P. aeruginosa* (1.6 versus 2.3 μM, respectively) (Table 3). However, increasing the number of hydrophobic interactions on the non-polar face increased hemolytic activity by 3-fold (HC_{50} from 254.1 μM for peptide **D11** to 81.3 μM for peptide **D22**) and thus decreased the therapeutic index greater than 4-fold for both Gram-negative pathogens (423.5 for **D11** to 101.6 for **D22** against *A. baumannii*, and 158.8 for **D11** to 35.3 for **D22** against *P. aeruginosa*) (Table 4). Thus, peptide **D11** has a significant improvement over peptide **D22** and **D1 (K13)** described earlier (Table 4). These results suggest that increasing hydrophobicity of **D22** compared to that of **D11** increased hemolytic activity and decreased the therapeutic index.

Peptide D22 versus peptide D14

These peptides were designed to be identical on both the polar and non-polar face, except that peptide **D14** has two specificity determinants (K13/K16), while peptide **D22** has only one specificity determinant (K13) (Figure 2). Both peptides have two clusters of large hydrophobes on both N- and C-terminus of their non-polar face: W2, F5, L6, F9 and L17, L20, L21, I24. The only difference on the non-polar face is the change of A16 in peptide **D22** to K16 in peptide **D14**.

K16, the second specificity determinant on peptide D14 decreased overall hydrophobicity by 8.9 min (Table 2) while maintaining the same hydrophobic interactions. This important substitution also lowered the amphipathicity (6.07 to 5.92) and association parameter from 5.13 for peptide D22 to 3.07 for peptide D14 similar to the association parameter of peptide D11 (3.31).

In our previous study, we showed that a single valine-to-lysine substitution in the center of non-polar face (V13K) dramatically reduced toxicity and increased the therapeutic index (8). Comparing peptides **D22** and **D14**, an extra Ala-to-Lys substitution generated a second specificity determinant, which maintained the same level of antimicrobial activity, but had a large improvement (i.e. decrease) in hemolytic activity (351.5 μM HC_{50} value for peptide **D14** compared to 81.3 μM HC_{50} value for peptide **D22**), thereby increasing the therapeutic index by 4-fold (439.4 for peptide **D14** and 101.6 for peptide **D22** against *A. baumannii* and 140.6 for peptide **D14** and 35.3 for peptide **D22** against *P. aeruginosa*) (Table 4). As a consequence, the second specificity determinant in peptide **D14** results in significant decrease (i.e. improvement) in therapeutic indices over peptide **D1 (K13)** and **D22** with **D14** having very similar properties to peptide **D11** (therapeutic indices of 439.4 for peptide **D14** and 423.5 for peptide **D11** against *A. baumannii* and 140.6 for peptide **D14** and 158.8 for **D11** against *P. aeruginosa*) (Table 4). In other words, if you enhance hydrophobicity (**D22** versus **D11**), it has a disadvantage in the therapeutic index, but this hydrophobicity can be maintained as long as a second specificity determinant is introduced to counter the effect of increased hydrophobicity and the therapeutic index can be restored (**D11** versus **D14**) (Figure 2 and Table 4).

Peptides D11 versus D15 and D14 versus D16

These peptides were designed to examine the effect of different types of hydrophobes and different locations of the hydrophobes (Figure 3). All the peptides discussed earlier have five different types of large hydrophobes in the non-polar face: tryptophan (position 2), phenylalanine (positions 5 and 9), valine (position 16), isoleucine (position 24), and leucine (positions 6, 17, and 21). To test the change in the type of hydrophobe, we modified peptide **D11** (with one specificity determinant) and **D14** (with two specificity determinants) by substituting all large hydrophobes (other than leucine) to leucine. Two new peptides **D15** and **D16** were generated. All the basic characteristics of **D11** and **D14** were maintained: net charge, number of specificity determinants, number of large hydrophobes, and number of hydrophobic interactions. Only the type of large hydrophobe was changed. Trp, Phe, Val, and Ile were changed to Leu to give 8 Leu residues on the non-polar face of peptides **D15** and **D16** (Figure 3).

The change to all Leu residues in peptides **D15** and **D16** had the following effects: (i) comparing peptide **D11** to **D15** (Figure 3) where both peptides have one specificity determinant (K13), the change in hydrophobicity is 7.6 min (85.4 min for peptide **D11** to 93.0 min for peptide **D15**) and (ii) the change in association parameter is 4.09 (3.31 for peptide **D11** increases to 7.40 for peptide **D15**) as expected because of the dramatic increase in overall hydrophobicity on the non-polar face. The similar change in hydrophobes to Leu residues in peptide **D16** versus peptide **D14** had the following effects. Both peptides have the same two specificity determinants K13 and K16 (Figure 3). However, the change in hydrophobicity by changing 1 Trp, 2 Phe, and 1 Ile residue to Leu residues had only a very small effect on overall hydrophobicity of 1.8 min (Table 2), which is 4-fold lower than that observed for peptides **D11** to **D15** earlier. The change in association parameter was 2.1 (from 3.07 for peptides **D14** to 5.17 for peptide **D16**), which is 2-fold lower than that observed for peptides **D11** to **D15** earlier. Thus, the change in hydrophobicity and association parameter is much greater in peptides **D11** to **D15** (analogs with one specificity determinant) than for peptides **D14** to **D16** (analogs with two specificity determinants). These results agree with the concept of specificity determinants, having two Lys residues instead of one in the center of the non-polar face decreases hydrophobicity and disrupts dimerization significantly more than one specificity determinant does even though the same 8 Leu residues exist in both **D15** and **D16** on the non-polar face.

This change in the type of hydrophobe had an interesting effect on hemolytic activity (Table 4). Hemolytic activity decreased from

254.1 μM HC_{50} value for peptide **D11** to 169.6 μM HC_{50} value for peptide **D15**, which was expected with the overall increase in hydrophobicity on **D15** from the increased number of Leu residues (Figure 3 and Table 2). However, the increase in hydrophobicity had the opposite effect with peptide **D16** showing a 3.8-fold improvement (i.e. decrease) in hemolytic activity compared to **D14** (1342 μM HC_{50} value for peptide **D16** versus 351.5 μM HC_{50} value for peptide **D14**). The change in type of hydrophobe to Leu residues had no significant effect on antimicrobial activity against *A. baumannii* (0.6 μM MIC_{GM} value for peptide **D11** to 0.5 μM MIC_{GM} value for peptide **D15**), while there was a 2-fold improvement in antimicrobial activity in changing to all Leu residue in **D16** compared peptide **D14** (0.8 μM MIC_{GM} value) to **D16** (0.4 μM MIC_{GM} value) against *A. baumannii* (Table 3). In the case of *P. aeruginosa*, the change from peptide **D11** to **D15** (1.6–1.0 μM of MIC_{GM} value, respectively) was similar to the change from peptide **D14** to **D16** (2.5–1.5 μM of MIC_{GM}, respectively). The huge decrease in hemolytic activity made **D16** the best among these four analogs: therapeutic index against *A. baumannii* for **D16** was 3355, while **D11**, **D14**, and **D15** were 423.5, 439.4, and 339.2, respectively (Table 4). Similarly, the therapeutic index against *P. aeruginosa* for **D16** was 894.7 while **D11**, **D14** and **D15** were 158.8, 140.6, 169.6, respectively. There was an 8- to 10-fold improvement in the therapeutic index for **D16** compared to **D11**, **D14**, and **D15** against *A. baumannii* and a 5- to 6-fold improvement in the therapeutic index for **D16** compared to **D11**, **D14**, and **D15** against *P. aeruginosa* (Table 4).

Discussion

We have shown that there are three important characteristics that affect the activity profile of amphipathic α-helical antimicrobial peptides: (i) the number and location of the positively charged residues on the polar face of the molecule; (ii) the number and location of the hydrophobic residues on the non-polar face including their hydrophobicity and type of hydrophobe; and (iii) the location and number of 'specificity determinant(s)' on the non-polar face.

The net positive charge is a very important characteristic affecting the activity of AMPs. The positively charged AMPs are attracted to the negatively charged surface of the microorganism to interact with the negatively charged phospholipids on the cell membrane. Structure–activity studies showed that increasing net positive charge without changing the length of the peptide maintained or increased antimicrobial activity without increasing hemolytic activity (41–43). In our previous studies, we used V13K as a lead compound to systematically decrease and increase the net positive charge on the polar face by varying the number of positively charged residues from 0 to 10 and the number of negatively charged residues from 0 to 6 in various combinations such that the net charge varied from −5 to +10. These results showed that the number of positively charged residues on the polar face and net charge are both important for antimicrobial activity and hemolytic activity (12).

In a follow-up study, we examined the effect of net positive charge and location of the positively charged residues on the polar face where the number of positively charged residues in the peptide varied from 5 to 10 (44). Based on these results, we selected the following polar face for the present study: a cluster of four positively charged residues in the center of the polar face (K11, K14, K15, and K18) plus an extended narrow strip of positively charged residues K3 and K7 at the N-terminal end of the polar face and K22 and K26 at the C-terminal end of the polar face (Figure 2 and Figure 3). The dramatic change of the location of the positively charged lysine residues and the increase of net charge from +7 for peptide **D1 (K13)** to +10 for peptide **D11** decreased hemolytic activity while increasing antimicrobial activity resulting in a 3.3- to 4.6-fold improvement in therapeutic indices against the two Gram-negative pathogens compared to peptide **D1 (K13)** (Table 4). Because the non-polar faces on peptides **D1 (K13)** and **D11** are identical (Figure 2), these results clearly show that the number of positively charged residues and their location on the polar face can have a large effect on hemolytic and antimicrobial activity resulting in a large improvement in the therapeutic index.

The number, location, and type of hydrophobic residues on the non-polar face and their effect on overall hydrophobicity of the peptide are other important characteristics affecting the activity of AMPs. Amphipathic α-helical AMPs must have a certain minimum hydrophobicity to penetrate into the hydrophobic membrane of prokaryotic and eukaryotic cells. It is generally accepted that increasing the hydrophobicity of the non-polar face of amphipathic α-helical antimicrobial peptides would increase the hemolytic activity (11,45,46). In our previous research, we investigated the role of hydrophobicity of the non-polar face and showed that there was an optimum hydrophobicity on the non-polar face required to obtain the best therapeutic index (11). Increases in hydrophobicity beyond this optimum resulted in a dramatic reduction in antimicrobial activity, which correlated with an increase in peptide self-association. High hydrophobicity on the non-polar face will cause stronger peptide dimerization/oligomerization in solution, which in turn results in the monomer–dimer/oligomer equilibrium favoring the dimer/oligomer conformation. Peptide dimers/oligomers in their folded α-helical conformation are much larger in size than an unstructured monomer and could be inhibited from passing through the capsule and cell wall of microorganisms to reach the target membranes. This would explain the decrease in antimicrobial activity beyond the optimum hydrophobicity (11). On the other hand, increasing hydrophobicity on the non-polar face is directly related to increased toxicity in eukaryotic cells or increased hemolytic activity of human red blood cells (11) because there is no capsule or cell wall in eukaryotic cells to prevent their access to the cytoplasmic membrane. In this study, **D11** and **D22** have identical polar faces and differ only in the location of the hydrophobes (Figure 2). **D11** and **D22** both have an N-terminal hydrophobic cluster consisting of W2, F5, L6, and F9 and only differ in the C-terminal of the non-polar face (Figure 2). **D22** has a 4-residue hydrophobic cluster of L17, L20, L21, and I24, which can interact by i to $i + 3$/i to $i + 4$ hydrophobic interactions (four hydrophobic interactions), whereas **D11** does not have the same hydrophobic cluster. The four hydrophobes in **D11** provide only two hydrophobic interactions and the overall peptide is less hydrophobic (V16 in **D11** and L20 in **D22**). This subtle change in location of the hydrophobes results in a dramatic increase hemolytic activity for **D22** compared to **D11** and a resulting decrease in the therapeutic index by 4- to 5-fold (Table 4). Thus, the location of hydro-

phobes and overall hydrophobicity play an important role in achieving the desired activity profile for an amphipathic α-helical AMP.

If we compare peptides **D11** and **D15**, which have identical polar faces and the hydrophobes are located in the identical positions on the non-polar faces, the only difference between the two peptides is the change in type of hydrophobe. **D11** has 1 Trp, 2 Phe, 1 Val, and 1 Ile residue, which are changed to Leu residues in **D15** (Figure 3). This change increases the overall hydrophobicity of **D15** relative to **D11** and increases hemolytic activity of **D15** as expected. Thus, the therapeutic index for **D15** is worse than **D11** against *A. baumannii*. On the other hand, **D15** is more active than **D11** against *P. aeruginosa*, which results in similar therapeutic indices (Table 4). Clearly, the type of hydrophobe can affect both hemolytic and antimicrobial activity and the resulting effect on the therapeutic index is dependent on the organism. In a similar manner, compare peptides **D14** and **D16** (Figure 3), which have identical polar faces and non-polar faces with the only difference the change of 1 Trp, 2 Phe, and 1 Ile residue to Leu residues. In this case, the change of hydrophobes had little effect on overall hydrophobicity (Table 2), but had a dramatic effect on hemolytic activity (3.8-fold improvement for **D16**, Table 4), an improved effect on antimicrobial activity resulting in a large effect on the therapeutic index of 7.6-fold against *A. baumanni* and a 6.4-fold against *P. aeruginosa*. These results show that very similar sequence changes in **D11** to **D15** and **D14** to **D16** (Figure 3) can have dramatically different effects. The differences between **D11/D15** and **D14/D16** lie in the arrangement of the hydrophobes in the C-terminal of the peptides on the non-polar face and the incorporation of one specificity determinant in the D11/D15 pair and two specificity determinants in the **D14/D16** pair.

In support of our results that changing the type of hydrophobe can have very significant effects on the activity profile of an AMP are the results of Hawrani *et al.* (9) who showed that a single Phe-to-Trp substitution on the non-polar face significantly enhanced peptide binding to neutral membranes (100% phosphatidylcholine, a mimic of eukaryotic membranes). These results suggest that removal of Trp residues from AMPs might be an additional strategy for reducing eukaryotic cell toxicity and in our case removal of aromatics in general (1 Trp and 2 Phe residues) maybe responsible for reducing eukaryotic cell toxicity for peptide **D16**. Interestingly, Avrahami *et al.* (47) used *de novo* designed peptide analogs with the sequence KXXXKWXXKXXK (where X = Val, Ile, or Leu) to show that if X is all Leu, the analog has the highest hemolytic activity and is active against most of the bacteria tested, while if X is all Val or all Ile, the analogs have lower hemolytic activity but are only active against select bacteria. Their results are directly opposite to ours where all Leu residues on the non-polar face (**D16**, Figure 3) had the most desirable properties, extremely low hemolytic activity, excellent Gram-negative antimicrobial activity and unprecedented therapeutic indices (Table 4). These observations suggest that our 26-residue AMPs may be dramatically different than shorter antimicrobial peptides.

The 'specificity determinant(s)' design concept was developed in our laboratory and refers to positively charged residue(s) in the center of the non-polar face of amphipathic α-helical antimicrobial peptides to create selectivity between eukaryotic and prokaryotic membranes, that is, antimicrobial activity is maintained and hemolytic activity or cell toxicity to mammalian cells is decreased or eliminated (8,10–14). Our results with specificity determinants have been recently validated by other groups (9,46). Hawrani *et al.* (9) showed that peptide RTA3 (a 16-residue amphipathic α-helical AMP isolated from Gram-positive bacteria *Streptococcus mitis*) with Arg at position 5 in the center of non-polar face, lowered the hemolytic activity by 20-fold, while maintaining the same level of antimicrobial activity compared to the analog with Leu at position 5. Conlon *et al.* (46) showed that substituting Lys to Leu at position 16 in the center of non-polar face of peptide B2RP (a 21-residue α-helical AMP isolated from mink frog *Lithobates septentrionalis*) increased hemolytic activity by 5-fold without changing antimicrobial activity.

In this study, we designed antimicrobial peptides with identical polar and non-polar faces with the only change being the presence of one specificity determinant at position 13 (K13) or two specificity determinants at positions 13 and 16 (K13, K16), for example, comparison of **D22** and **D14** (Figure 2). Peptide **D22** has K13 and A16 and **D14** has K13 and K16 in the center of the non-polar face (Figure 2). The advantage of the second specificity determinant is that the hemolytic activity of **D14** is decreased by 4.3-fold compared to **D22** (Table 4) and the resulting therapeutic indices for **D14** against *A. baumannii* and *P. aeruginosa* were 4.3-fold and 4.0-fold better, respectively. Thus, if one increases the hydrophobicity on the non-polar face (compare **D11** to **D22**) (Figure 2), hemolytic activity increases; however, this can be overcome by inserting a second specificity determinant that decreases hemolytic activity (**D14**) (Table 4). With the correct combination of positively charged residues (number and location) on the polar face, the correct combination of number, location, and type of hydrophobe on the non-polar face, overall hydrophobicity and the correct number of specificity determinants antimicrobial peptides with the desired properties can be rationally designed.

The goal of this study, was to determine whether it was possible to further enhance the therapeutic indices of our lead peptide **D1 (K13)** if we focused our studies on Gram-negative bacteria only (*A. baumannii* and *P. aeruginosa*) rather than attempting to develop a broad-spectrum compound with activity against Gram-negative, Gram-positive bacteria, fungi, and *Mycobacterium tuberculosis* (8,10–14). Peptides **D11**, **D14**, **D15**, and **D16** all have significant improvements in therapeutic indices compared to our lead peptide **D1 (K13)** with peptide **D16** emerging as our most promising compound with unprecedented properties. In Figure 7, we have compared the sequences and structure of **D1 (V13)** original starting peptide, **D1 (K13)** our lead peptide with broad-spectrum activity to our new lead antimicrobial peptide, **D16** for treatment of Gram-negative infection. **D16** is totally different than **D1 (V13)**. The number of lysine residues and their location on the polar face are dramatically different. **D1 (V13)** has a net positive charge of +6, and **D1 (K13)** has a net positive charge of +7 compared to **D16** with a net charge of +11. The lysine residues in **D16** are organized to establish a cluster of four positively charged residues in the center of the polar face (K11, K14, K15 and K18), plus an extended narrow strip of positively charged residues (K3 and K7 at the N-ter-

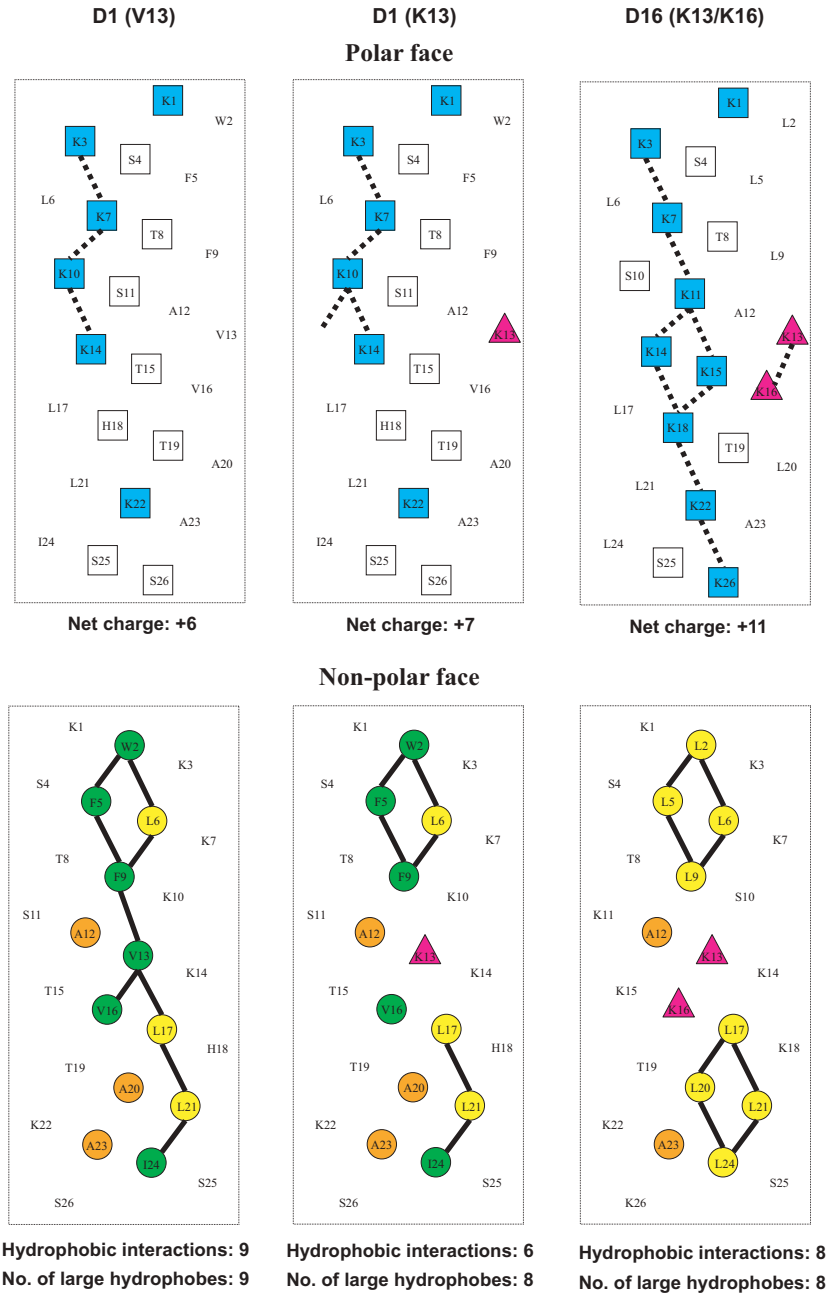

Figure 7: Helical net representations of peptides **D1 (V13)**, **D1 (K13)**, and **D16**. In the helical nets, the one-letter code is used for amino acid residues. The 'specificity determinant(s)' lysine residues at position 13 only or at positions 13 and 16 in the center of the non-polar face is denoted by a pink triangle(s). The amino acid residues on the polar face are boxed, and the positively charged lysine residues are colored blue. The potential $i \rightarrow i + 3$ and $i \rightarrow i + 4$ electrostatic repulsions between positively charged residues along the helix are shown as dotted bars. The amino acid residues on the non-polar face are circled; the large hydrophobes other than leucine residues (Trp, Phe, Val, and Ile) are colored green and the leucine residues are colored yellow; the alanine residues (A12, A20, and A23 in **D1**; A12 and A23 in **D16**) are colored orange. The $i \rightarrow i + 3$ and $i \rightarrow i + 4$ hydrophobic interactions between large hydrophobes along the helix are shown as black bars.

minal of the polar face and K22 and K26 at the C-terminal of polar face). On the non-polar face, **D1 (V13)** has an uninterrupted hydrophobic face with 9 i to $i + 3/i$ to $i + 4$ hydrophobic interactions among large hydrophobes. This hydrophobic surface is disrupted in peptide **D1 (K13)** with the introduction of a single specificity determinant K13. This specificity determinant reduces toxicity by 78-fold (Table 4). The effect of introducing a second specificity determinant (compare **D22** and **D14** (Figure 2)) reduced the HC_{50} value by 4.3-fold or a combined effect of 195-fold on the HC_{50} value compared to **D1 (V13)** with no specificity determinant

(Table 4). The non-polar face of **D16** has two hydrophobic clusters of Leu residues at positions 2, 5, 6, and 9 and 17, 20, 21, and 24 to create two hydrophobic patches separated by the two specificity determinants (K13 and K16). Although **D1** has the same four-residue hydrophobic cluster at the N-terminal as **D16** the hydrophobes in **D1** consist of Trp2, Phe5, Leu6, and Phe9 rather than 4 Leu residues in **D16**. **D1** in the C-terminal of the non-polar face has two Leu residues in common with **D16**, Leu17, and Leu21 but has V16, A20, and Ile 24 compared to Leu20 and Leu24 in **D16** (Figure 7). All these changes on the polar face and non-polar face of **D16** compared to **D1 (V13)** (Table 4) resulted in a combined effect on hemolytic activity of a 746-fold decrease (Table 4) and unprecedented improvements in the therapeutic indices of 1305-fold and 895-fold against *A. baumannii* and *P. aeruginosa*, respectively (Table 4).

In conclusion, our data suggest that peptide **D16** is an ideal antimicrobial peptide for further *in vivo* safety and efficacy studies in animal models and ultimately for its commercialization as a therapeutic agent for the treatment of human infections caused by these opportunistic Gram-negative pathogens.

Acknowledgments

This research was supported by a NIH grant from the National Institute of Allergy and Infectious Diseases (NIAID) R01 AI067296 (R.S.H.), the John Stewart Chair in Peptide Chemistry to R.S.H and the Department of Defense, Office of Naval Research through a STTR grant to BioAmps International Inc. The content is solely the responsibility of the authors and does not necessarily represent the official views of NIAID or NIH.

References

1. Gaynes R., Edwards J.R. (2005) Overview of nosocomial infections caused by gram-negative bacilli. Clin Infect Dis;41:848–854.
2. Maragakis L.L., Perl T.M. (2008) Acinetobacter baumannii: epidemiology, antimicrobial resistance, and treatment options. Clin Infect Dis;46:1254–1263.
3. Rice L.B. (2006) Challenges in identifying new antimicrobial agents effective for treating infections with Acinetobacter baumannii and Pseudomonas aeruginosa. Clin Infect Dis;43(Suppl 2):S100–S105.
4. Hancock R.E. (1998) Resistance mechanisms in Pseudomonas aeruginosa and other nonfermentative gram-negative bacteria. Clin Infect Dis;27(Suppl 1):S93–S99.
5. Garza-Gonzalez E., Llaca-Diaz J.M., Bosques-Padilla F.J., Gonzalez G.M. (2010) Prevalence of multidrug-resistant bacteria at a tertiary-care teaching hospital in Mexico: special focus on Acinetobacter baumannii. Chemotherapy;56:275–279.
6. Hancock R.E., Lehrer R. (1998) Cationic peptides: a new source of antibiotics. Trends Biotechnol;16:82–88.
7. Hodges R.S., Jiang Z., Whitehurst J., Mant C.T. (in press) Development of antimicrobial peptides as therapeutic agents. In: Gad S., Eventhal M., editors. Development of Therapeutic Agents, Handbook in Pharmaceutical Sciences. Hoboken, NJ: John Wiley and Sons.
8. Chen Y., Mant C.T., Farmer S.W., Hancock R.E., Vasil M.L., Hodges R.S. (2005) Rational design of alpha-helical antimicrobial peptides with enhanced activities and specificity/therapeutic index. J Biol Chem;280:12316–12329.
9. Hawrani A., Howe R.A., Walsh T.R., Dempsey C.E. (2008) Origin of low mammalian cell toxicity in a class of highly active antimicrobial amphipathic helical peptides. J Biol Chem;283:18636–18645.
10. Chen Y., Vasil A.I., Rehaume L., Mant C.T., Burns J.L., Vasil M.L., Hancock R.E., Hodges R.S. (2006) Comparison of biophysical and biologic properties of alpha-helical enantiomeric antimicrobial peptides. Chem Biol Drug Des;67:162–173.
11. Chen Y., Guarnieri M.T., Vasil A.I., Vasil M.L., Mant C.T., Hodges R.S. (2007) Role of peptide hydrophobicity in the mechanism of action of alpha-helical antimicrobial peptides. Antimicrob. Agents Chemother;51:1398–1406.
12. Jiang Z., Vasil A.I., Hale J.D., Hancock R.E., Vasil M.L., Hodges R.S. (2008) Effects of net charge and the number of positively charged residues on the biological activity of amphipathic alpha-helical cationic antimicrobial peptides. Biopolymers (Peptide Science);90:369–383.
13. Jiang Z., Kullberg B.J., van der Lee H., Vasil A.I., Hale J.D., Mant C.T., Hancock R.E.W., Vasil M.L., Netea M.G., Hodges R.S. (2008) Effects of Hydrophobicity on the Antifungal Activity of a-Helical Antimicrobial Peptides. Chem Biol Drug Des;72:483–495.
14. Jiang Z., Hggins M.P., Whitehurst J., Kisich K.O., Voskuil M.I., Hodges R.S. (2011) Anti-tuberculosis activity of alpha-helical antimicrobial peptides: de novo designed L- and D-enantiomers versus L- and D-LL-37. Protein Pept Lett; PMID: 20858205. (in press).
15. Chen Y., Mant C.T., Hodges R.S. (2007) Preparative reversed-phase high-performance liquid chromatography collection efficiency for an antimicrobial peptide on columns of varying diameters (1mm to 9.4mm I.D.). J Chromatogr A;1140:112–120.
16. Lee D.L., Mant C.T., Hodges R.S. (2003) A novel method to measure self-association of small amphipathic molecules: temperature profiling in reversed-phase chromatography. J Biol Chem;278:22918–22927.
17. Eisenberg D., Weiss R.M., Terwilliger T.C. (1982) The helical hydrophobic moment: a measure of the amphiphilicity of a helix. Nature;299:371–374.
18. Carver T., Bleasby A. (2003) The design of Jemboss: a graphical user interface to EMBOSS. Bioinformatics;19:1837–1843.
19. Kovacs J.M., Mant C.T., Hodges R.S. (2006) Determination of intrinsic hydrophilicity/hydrophobicity of amino acid side chains in peptides in the absence of nearest-neighbor or conformational effects. Biopolymers (Peptide Science);84:283–297.
20. Mant C.T., Kovacs J.M., Kim H.M., Pollock D.D., Hodges R.S. (2009) Intrinsic amino acid side-chain hydrophilicity/hydrophobicity coefficients determined by reversed-phase high-performance liquid chromatography of model peptides: comparison with other hydrophilicity/hydrophobicity scales. Biopolymers (Peptide Science);92:573–595.
21. Holloway B.W. (1955) Genetic recombination in Pseudomonas aeruginosa. J Gen Microbiol;13:572–581.

22. Bjorn M.J., Vasil M.L., Sadoff J.C., Iglewski B.H. (1977) Incidence of exotoxin production by Pseudomonas species. Infect Immun;16:362–366.
23. Pavlovskis O.R., Pollack M., Callahan L.T. III, Iglewski B.H. (1977) Passive protection by antitoxin in experimental Pseudomonas aeruginosa burn infections. Infect Immun;18:596–602.
24. Frost L.S., Paranchych W. (1977) Composition and molecular weight of pili purified from Pseudomonas aeruginosa K. J Bacteriol;131:259–269.
25. Watts T.H., Kay C.M., Paranchych W. (1982) Dissociation and characterization of pilin isolated from Pseudomonas aeruginosa strains PAK and PAO. Can J Biochem;60:867–872.
26. Rahme L.G., Ausubel F.M., Cao H., Drenkard E., Goumnerov B.C., Lau G.W., Mahajan-Miklos S., Plotnikova J., Tan M.W., Tsongalis J., Walendziewicz C.L., Tompkins R.G. (2000) Plants and animals share functionally common bacterial virulence factors. Proc Natl Acad Sci U S A;97:8815–8821.
27. Stieritz D.D., Holder I.A. (1975) Experimental studies of the pathogenesis of infections due to Pseudomonas aeruginosa: description of a burned mouse model. J Infect Dis;131:688–691.
28. Chen H.C., Brown J.H., Morell J.L., Huang C.M. (1988) Synthetic magainin analogues with improved antimicrobial activity. FEBS Lett;236:462–466.
29. Mor A., Nicolas P. (1994) The NH2-terminal alpha-helical domain 1-18 of dermaseptin is responsible for antimicrobial activity. J Biol Chem;269:1934–1939.
30. Blazyk J., Wiegand R., Klein J., Hammer J., Epand R.M., Epand R.F., Maloy W.L., Kari U.P. (2001) A novel linear amphipathic beta-sheet cationic antimicrobial peptide with enhanced selectivity for bacterial lipids. J Biol Chem;276:27899–27906.
31. Chekmenev E.Y., Vollmar B.S., Forseth K.T., Manion M.N., Jones S.M., Wagner T.J., Endicott R.M. *et al.* (2006) Investigating molecular recognition and biological function at interfaces using piscidins, antimicrobial peptides from fish. Biochim Biophys Acta;1758:1359–1372.
32. Gibson B.W., Tang D.Z., Mandrell R., Kelly M., Spindel E.R. (1991) Bombinin-like peptides with antimicrobial activity from skin secretions of the Asian toad, Bombina orientalis. J Biol Chem;266:23103–23111.
33. Conlon J.M., Sonnevend A., Davidson C., Smith D.D., Nielsen P.F. (2004) The ascaphins: a family of antimicrobial peptides from the skin secretions of the most primitive extant frog, Ascaphus truei. Biochem Biophys Res Commun;320:170–175.
34. Shin S.Y., Hahm K.S. (2004) A short alpha-helical antimicrobial peptide with antibacterial selectivity. Biotechnol Lett;26:735–739.
35. Tencza S.B., Douglass J.P., Creighton D.J. Jr, Montelaro R.C., Mietzner T.A. (1997) Novel antimicrobial peptides derived from human immunodeficiency virus type 1 and other lentivirus transmembrane proteins. Antimicrob Agents Chemother;41:2394–2398.
36. Chen Y., Mant C.T., Hodges R.S. (2002) Determination of stereochemistry stability coefficients of amino acid side-chains in an amphipathic alpha-helix. J Pept Res;59:18–33.
37. Zhou N.E., Mant C.T., Hodges R.S. (1990) Effect of preferred binding domains on peptide retention behavior in reversed-phase chromatography: amphipathic alpha-helices. Pept Res;3:8–20.
38. Mant C.T., Chen Y., Hodges R.S. (2003) Temperature profiling of polypeptides in reversed-phase liquid chromatography. I. Monitoring of dimerization and unfolding of amphipathic alpha-helical peptides. J Chromatogr A;1009:29–43.
39. Mant C.T., Tripet B., Hodges R.S. (2003) Temperature profiling of polypeptides in reversed-phase liquid chromatography. II. Monitoring of folding and stability of two-stranded alpha-helical coiled-coils. J Chromatogr A;1009:45–59.
40. Dolan J.W. (2002) Temperature selectivity in reversed-phase high performance liquid chromatography. J Chromatogr A;965:195–205.
41. Yang Y.X., Feng Y., Wang B.Y., Wu Q. (2004) PCR-based site-specific mutagenesis of peptide antibiotics FALL-39 and its biologic activities. Acta Pharmacol Sin;25:239–245.
42. Dathe M., Nikolenko H., Meyer J., Beyermann M., Bienert M. (2001) Optimization of the antimicrobial activity of magainin peptides by modification of charge. FEBS Lett;501:146–150.
43. Ahn H.S., Cho W., Kang S.H., Ko S.S., Park M.S., Cho H., Lee K.H. (2006) Design and synthesis of novel antimicrobial peptides on the basis of alpha helical domain of Tenecin 1, an insect defensin protein, and structure-activity relationship study. Peptides;27:640–648.
44. Jiang Z., Vasil A.I., Vasil M.L., Hodges R.S. (2010) Effect of Net Positive Charge and Charge Distribution on the Polar Face of Amphipathic α-Helical Antimicrobial Peptides on their Biological and Biophysical Properties. In Lebl M.., editors. Breaking Away: Proceedings of the 21st American Peptide Symposium (2009), Bloomington, IN, USA: American Peptide Society, pp. 266–267.
45. Asthana N., Yadav S.P., Ghosh J.K. (2004) Dissection of antibacterial and toxic activity of melittin: a leucine zipper motif plays a crucial role in determining its hemolytic activity but not antibacterial activity. J Biol Chem;279:55042–55050.
46. Conlon J.M., Ahmed E., Condamine E. (2009) Antimicrobial properties of brevinin-2-related peptide and its analogs: efficacy against multidrug-resistant Acinetobacter baumannii. Chem Biol Drug Des;74:488–493.
47. Avrahami D., Oren Z., Shai Y. (2001) Effect of multiple aliphatic amino acids substitutions on the structure, function, and mode of action of diastereomeric membrane active peptides. Biochemistry;40:12591–12603.